

CONTROL ALGORITHM TESTS USING A VIRTUAL CW SRF CAVITY

Josu Jugo*, Ander Elejaga, University of the Basque Country UPV/EHU, Leioa, Spain
Pablo Echevarria, Helmholtz Zentrum Berlin, Berlin, Germany

Abstract

Superconducting cavities (SRF) are widely used in new generation particle accelerators, increasing the requirements and specifications for new designs. The LLRF control system, including the detuning control due to mechanical perturbations, must fulfill more exigent specifications, and its design have gained increasing relevance. The Helmholtz Zentrum Berlin, among others, have been working in the development of simulation and Hardware-in-the-loop tools to facilitate the test of control algorithms. The main goal of this work is to use an existing cavity model in CW mode, a Tesla cavity including a Saclay style piezo-tuner, and simulation tools to compare and test different control strategies focused in the detuning reduction, specially microphonics. The design process consist of the use of pure simulation environment based on Matlab/Simulink, where the mathematical model includes a cavity model, a LLRF control system and detuning control strategies, considering the mentioned actuator. Different control strategies are considered for the RF and mechanical parts: perturbation reduction by PID based feedback loops, adaptive feedforward algorithms, and active disturbance rejection techniques (ADRC). The aim is the performance comparison of the different algorithms with different perturbations, by using realistic cavity models which include Lorentz force detuning, microphonics derived from the cryogenic module and so forth. The simulation environment allows the inclusion of other effects as the non-collocated control problem.

INTRODUCTION

The use of simulation models and Hardware-in-the-loop (HIL) techniques for developing virtual cavities is a relevant tool for the setting up and debugging of cavities' support systems, [1–5]. This includes the analysis, design and test of LLRF control systems, quench detection, resonance frequency control among others, resulting in a reduction of the otherwise time consuming and costly operation of real cavities.

On the other hand, simulation and HIL models are complementary. Simulation models allow a versatile working environment for rapid test and comparison of different ideas and proposal [1], while FPGA-based virtual cavities allow the use of real hardware implementations, given a more realistic picture of the system performance [2–4] (including forward and reverse RF signal, quenching, field dependent Q_0 , Lorentz force detuning and microphonics) and the possibility of a quasi automatic interchange of virtual and real cavities. However, the implementation of the algorithms in a HIL system requires an extra effort comparing with a

	Q_o	$R/Q(\Omega)$	$f_{RF} GHz$
Tesla cavity	$5.0 \cdot 10^{10}$	900	1.3

Table 1: Main parameters of Tesla cavity

	Mode 1	Mode 2	Mode 3	Mode 4
ω_n	262	589	1079	1216
damping δ	0.0025	0.0045	0.0036	0.0047
Lorentz coupling (Hz/(MV/m) ²)	0.5	0.5	0.5	0.5
Piezo coupling (Hz/V)	-0.008	0.048	-0.052	0.038

Table 2: Main mechanical modes of Tesla cavity

simulation environment. As conclusion, in a first phase, the use of simulated virtual cavities are useful for an agile test and comparison of multiple ideas and algorithms and, in a second phase, the most promising ones can be tested in a HIL system, to validate the obtained results.

In this work, a simulated virtual TESLA cavity in CW mode [6,7] and LLRF system is used in order to test different control algorithm, for the stabilization of the RF signal and for the frequency resonance perturbation reduction. In particular, three control algorithms are implemented: a standard PID control, an active disturbance rejection control (ADRC) algorithm [8, 10] and an adaptive feedforward controller [9]. Different combinations of such control algorithms are used in the two control loops: the RF control and the resonance frequency control loop. The cavity model considered in this study as reference describes mainly a Tesla cavity from HZB.

Using different control scheme combinations, the effect of the interaction between the two control loops can be also analyzed, since the relevance of such interaction has also been reported in previous works. The presented results show that this framework will be useful to study different control strategies and problems, and encourage to perform more detailed tests.

SYSTEM DESCRIPTION

The simulations are based in the use of a 9-cell Tesla cavity model implemented in a MATLAB/Simulink environment, whose basic electric parameters are shown in Table 1, being Q_o the quality factor of the cavity, R/Q represent the efficiency of the acceleration process which is dependent on the cavity's geometry and f_{RF} is the nominal resonant frequency of the cavity. Additionally, the Table 2 shows the main mechanical modes of the cavity (20 modes in total).

The scheme of the simulation system is depicted in Figure 1. The system includes the electrical and mechanical model of the cavity, the RF part (Klystron and coupling) and a piezo tuner, considering a time delay and the mechanical effect

* corresponding author

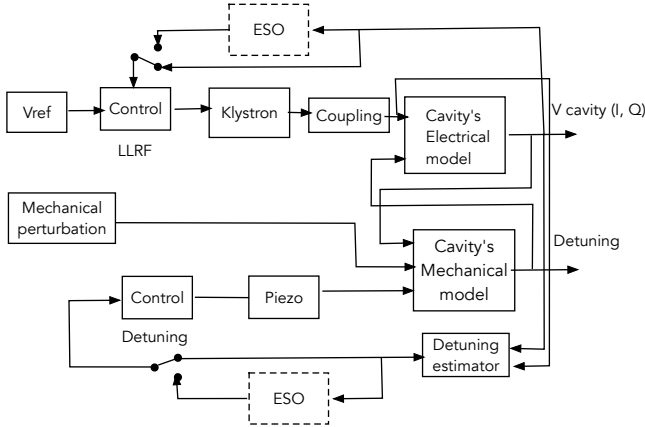


Figure 1: Simplified simulation scheme, including Klystron, coupling and cavity's electrical and mechanical model. The observer blocks (ESO) are used for the ADRC controllers.

of such tuner in the cavity. The impact of the tuner delay is discussed in the Simulation results Section. Additionally, the differences between the mechanical dynamics of the cavity and the piezo allow the study of the non-collocated control problem. The non-collocated control problem appears when the sensor and the actuator are placed in different positions. In this case, the cavity acts as the sensor, translating the mechanical perturbations to the RF part. On the other hand, the piezo-tuner is positioned in a particular place, which can lead to controllability issues.

IMPLEMENTED CONTROL ALGORITHMS

The implemented system has two main control loops. The first one is the principal LLRF system for the control of the RF signal in amplitude and in phase, using an I/Q based approach. The second control loop is introduced for reducing the mechanical perturbations by mean of a piezo tuner.

LLRF control for the cavity field

Two algorithms are considered here for the comparison tests: a standard PI control and an ADRC algorithm.

PI control. The scheme of the discrete PI controller implemented is basic, described by the next expression:

$$g(z) = K_p + \frac{K_i T_s}{z - 1} \quad (1)$$

being $T_s = 1 \times 10^{-5} s$ the sampling period. In this case, the controller parameters are $K_p = 2 \times 10^{-6}$ and $K_i = 5 \times 10^{-3}$, designed initially using the first order model of the cavity filling and tuned by simulation. Two control loops are implemented for the real and imaginary parts of the RF signal, allowing the amplitude and phase control.

ADRC control. The ADRC controller is based on an Extended State Observer (ESO), which takes the measured process's input and output, and estimates the underlying

noise-free trend in real time. The ESO estimates the total disturbance acting on the system which is then fed back into the control scheme and cancelled via the ADRC law. As a result of this cancelation, the plant is reduced to its simplest form which can be easily controlled via proportional means.

Based on [12], an ADRC control algorithm has been developed and applied to this particular cavity model. The MIMO cavity equation can be expressed in matrix form as follows.

$$\begin{bmatrix} \dot{V}_{cr} \\ \dot{V}_{ci} \end{bmatrix} = \begin{bmatrix} -\omega_{1/2} & -\Delta\omega \\ -\Delta\omega & -\omega_{1/2} \end{bmatrix} \begin{bmatrix} V_{cr} \\ V_{ci} \end{bmatrix} + \frac{R_L \omega_{1/2}}{m} \begin{bmatrix} I_{rfr} \\ I_{rfi} \end{bmatrix} + \frac{R_L \omega_{1/2}}{m} \begin{bmatrix} I_{br} \\ I_{bi} \end{bmatrix} \quad (2)$$

where V_{cr} and V_{ci} are the real and imaginary part of the cavity voltage, $\omega_{1/2}$ is the half-bandwidth of the cavity, R_L is the load resistance, m is the ratio of the transformer and $\Delta\omega$ is the detuning. Furthermore, I_{rfr} , I_{rfi} , I_{br} and I_{bi} are the decomposition into real and imaginary part of the effective driving intensities for RF power and beam loading. Note that the aforementioned terms can be defined in the following way.

$$\mathbf{y} = \begin{bmatrix} V_{cr} \\ V_{ci} \end{bmatrix}, \mathbf{A} = \begin{bmatrix} -\omega_{1/2} & -\Delta\omega \\ -\Delta\omega & -\omega_{1/2} \end{bmatrix}, \mathbf{B}_0 = \frac{R_L \omega_{1/2}}{m},$$

$$\mathbf{u} = \begin{bmatrix} I_{rfr} \\ I_{rfi} \end{bmatrix}, \mathbf{d} = \begin{bmatrix} I_{br} \\ I_{bi} \end{bmatrix}$$

Being the beam loading viewed as a disturbance (\mathbf{d}), the cavity equation can be rewritten as

$$\dot{\mathbf{y}} = \mathbf{A}\mathbf{y} + \mathbf{B}_0\mathbf{u} + \mathbf{B}_0\mathbf{d} \quad (3)$$

If the system dynamics are considered as unknown perturbations, the equation can be rewritten as follows.

$$\dot{\mathbf{y}} = \mathbf{f} + \mathbf{B}_0\mathbf{u} \quad (4)$$

where \mathbf{f} is the general disturbance term that will be estimated by the ESO, and further on actively cancelled by the ADRC control. In this way, the two items to be estimated by the observer are $\hat{\mathbf{x}}_1 = \hat{\mathbf{y}}$ and $\hat{\mathbf{x}}_2 = \hat{\mathbf{f}}$. An observer can be defined to estimate those two parameters based on the input \mathbf{u} and output \mathbf{y} of the system:

$$\begin{bmatrix} \hat{\mathbf{x}}_1 \\ \hat{\mathbf{x}}_2 \end{bmatrix} = \begin{bmatrix} 0 & \mathbf{I} \\ 0 & 0 \end{bmatrix} \begin{bmatrix} \hat{\mathbf{x}}_1 \\ \hat{\mathbf{x}}_2 \end{bmatrix} + \mathbf{B}_0 \begin{bmatrix} \mathbf{I} \\ 0 \end{bmatrix} \mathbf{u} + \mathbf{L}(\mathbf{y} - \hat{\mathbf{x}}_1) \quad (5)$$

where \mathbf{L} is a parameter matrix that will determine the poles of the observer and hence, its dynamics [12]. Equation 5 can be rewritten in this particular case as

$$\begin{bmatrix} \dot{\hat{V}}_{cr} \\ \dot{\hat{V}}_{ci} \\ \dot{\hat{f}}_r \\ \dot{\hat{f}}_i \end{bmatrix} = \begin{bmatrix} -l_{11} & -l_{12} & 1 & 0 \\ -l_{21} & -l_{22} & 0 & 1 \\ -l_{31} & -l_{32} & 0 & 0 \\ -l_{41} & -l_{42} & 0 & 0 \end{bmatrix} \begin{bmatrix} \hat{V}_{cr} \\ \hat{V}_{ci} \\ \hat{f}_r \\ \hat{f}_i \end{bmatrix} + \begin{bmatrix} l_{11} & l_{12} & B_0 & 0 \\ l_{21} & l_{22} & 0 & B_0 \\ l_{31} & l_{32} & 0 & 0 \\ l_{41} & l_{42} & 0 & 0 \end{bmatrix} \begin{bmatrix} V_{cr} \\ V_{ci} \\ I_{rfr} \\ I_{rfi} \end{bmatrix}$$

The dynamics of the observer must be notably faster than the closed loop behavior of the cavity, so that the estimation and rejection of disturbances can be performed before they generate large perturbations in the EM fields. For this particular system all the poles have been placed at -3000 Hz and to do so, the \mathbf{L} matrix parameters have been determined as follows:

$$l_{12} = l_{21} = l_{32} = l_{41} = 0$$

$$l_{11} = l_{22} = 12000\pi$$

$$l_{31} = l_{42} = 36000000\pi^2$$

Regarding the controller, a proportional control and disturbance rejection can be implemented using the following control law

$$u = \frac{\mathbf{K}_p(\mathbf{r} - \hat{\mathbf{y}}) - \hat{\mathbf{f}}}{B_0} \quad (6)$$

being \mathbf{K}_p a 2x2 gain matrix and \mathbf{r} the set point voltage of the cavity in real and imaginary form.

Control of mechanical perturbations

Three different control algorithms are considered for the Lorenz force detuning and microphonics reduction: a standard PI feedback loop, an ADRC controller and an adaptive feedforward

With respect to the mechanical disturbances suffered by the system, two main sources have been considered. On the one hand, the cavity voltage, set at 9 MV, generates a Lorenz Force detuning of about 600 Hz. On the other hand, to simulate the effect of external microphonics, a white noise signal has been added to the mechanical model of the cavity, generating a random detuning in the range from -5 Hz to 5 Hz, with a RMS value of 1.7 Hz. Furthermore, a pure sinusoidal signal at 80 Hz has been added.

PI control. A discrete PI controller (Eq. 1) has been implemented as first choice. Similarly to the previous case, the controller has been tuned by simulation and its control parameters are $K_p = 0.55$ and $K_i = 20$.

ADRC control. The model of the mechanical dynamics introduced by the Saclay II piezo tuner used in this work has a relative order of one. This means that a first order extended state observer (ESO) is enough to implement the ADRC control [8, 11]. In this way, the parameters to be observed are the detuning $\Delta\omega$ and the total disturbance \hat{f} . Following the process exposed in the section above, the observer is defined by the next matrix equation.

$$\begin{bmatrix} \hat{\Delta\omega} \\ \hat{f} \end{bmatrix} = \begin{bmatrix} -l_1 & 1 \\ -l_2 & 0 \end{bmatrix} \begin{bmatrix} \Delta\omega \\ \hat{f} \end{bmatrix} + B_0 \begin{bmatrix} 1 & l_1 \\ 0 & l_2 \end{bmatrix} \begin{bmatrix} V_{piezo} \\ \Delta\omega \end{bmatrix} \quad (7)$$

where $\hat{\Delta\omega}$ and \hat{f} are the observed detuning and total disturbance, V_{piezo} is the voltage entering the piezo and l_1 and l_2

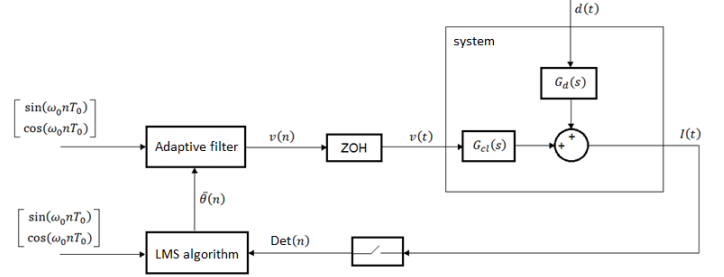


Figure 2: AFF control scheme

are the parameters that define the dynamics of the observer. In this particular case, it is considered that the piezo-tuner has a 114 μs mechanical delay, and trying to cancel every single disturbance would result in the destabilization of the controller, due to the inability of the actuator to respond in time to the fastest dynamics. In order to solve this issue, the poles of the observer have been placed at a relatively low frequency (50 Hz) to ensure that only the slowest disturbances are corrected. This is an important limitation of the implemented design. In this way, the \mathbf{L} matrix parameters are defined as $l_1 = 628$ and $l_2 = 98696$ and $B_0 = 3.5714 \times 10^{-05}$.

Adaptive Feedforward. To cope with constant frequency microphonics, such as those provoked by repetitive disturbances as vacuum pumps, an Adaptive Feedforward (AFF) control [9] has been tested. As it has been reported in previous work, this kind of controllers notably suppress located microphonics by computing and generating a sinusoidal control signal with the appropriate amplitude and phase to cancel the perturbation. In this manner, an AFF has been added to the existing PI and ADRC controllers to try and suppress a 80 Hz microphonic. The particular controller structure implemented, a filtered-x LMS algorithm, is shown in the Figure 2.

On the one hand, the LMS algorithm searches for the correct phase and amplitude of the control signal by implementing the following equations.

$$\begin{aligned} \bar{\theta}(n) &= [A_1(n), A_2(n)] \\ A_1(n) &= A_1(n-1) + \gamma \text{Det}(n) \sin(\omega_0 n T_0) \\ A_2(n) &= A_2(n-1) + \gamma \text{Det}(n) \cos(\omega_0 n T_0) \end{aligned} \quad (8)$$

being $\text{Det}(n)$ the detuning perturbation to reduce, T_0 is the AFF sampling rate and ω_0 the frequency of the perturbation. On the other hand, the adaptive filter generates a sine wave with the parameters obtained from the LMS algorithm.

$$v(n) = [A_1(n), A_2(n)] \begin{bmatrix} \sin(\omega_0 n T_0) \\ \cos(\omega_0 n T_0) \end{bmatrix} \quad (9)$$

SIMULATION RESULTS

Different scenarios have been considered, combining the control algorithms in the two loops, always in CW mode. Mainly, the next combinations have been tested:

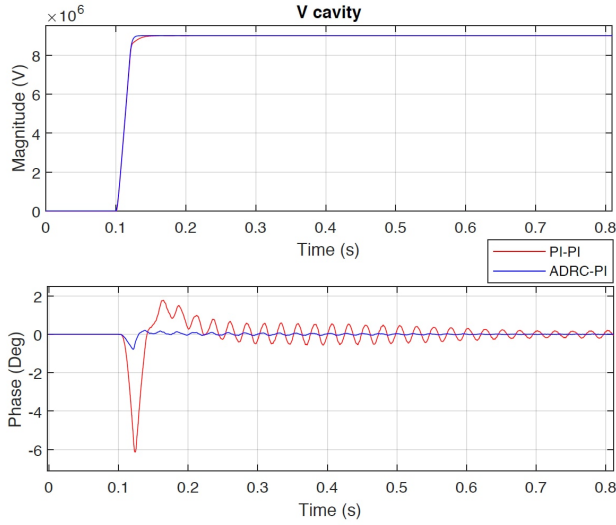


Figure 3: Time response of the cavity filling

- Scenario 1: A basic PI in the 1st and 2nd loops
- Scenario 2: An ADRC in the 1st loop and a PI controller in the 2nd loop
- Scenario 3: An ADRC in the 1st and 2nd loops
- Scenario 4: A PI controller in the 1st loop and an ADRC controller in the 2nd loop
- Scenario 5: An ADCR controller in the 1st loop and a PI controller and the adaptive feedforward controller in the 2nd loop

The figure 3 shows the cavity filling, representing the amplitude and phase behavior for the main two scenarios considered for the 1st loop: a standard PI and the ADCR control algorithm. As it is observed, the amplitude error is negligible in both cases, being faster the stabilization of the signal in the ADRC case. Most evident is the advantage of this control scheme observing the phase behavior, being the stabilization time very short and final error very low ($<0.01\text{Å}^\circ$). In this figure, only scheme 1 and 2 are shown, since the effect of the second control loop is negligible.

Figure 4 and 5 show the results obtained for the control of mechanical perturbations. Four different scenario are included. The results of the scheme 4 are not included since it has not been possible the obtaining of reasonable results. This problem is discussed below.

As it is observed in those figures, the best results are obtained with the basic PI controller in the tuner loop (Scheme 1, 2 or 5). The PI controller reduces the detuning, in the time domain, in a factor 5 (comparing with the open-loop case), with an approximated bandwidth of 350Hz. In figure 5, it is observed that the sinusoidal perturbation is cancelled by mean of the AFF feedforward algorithm (Scheme 5),

The ADRC algorithm has reported very good results comparing with PID algorithms in the literature. This is the case

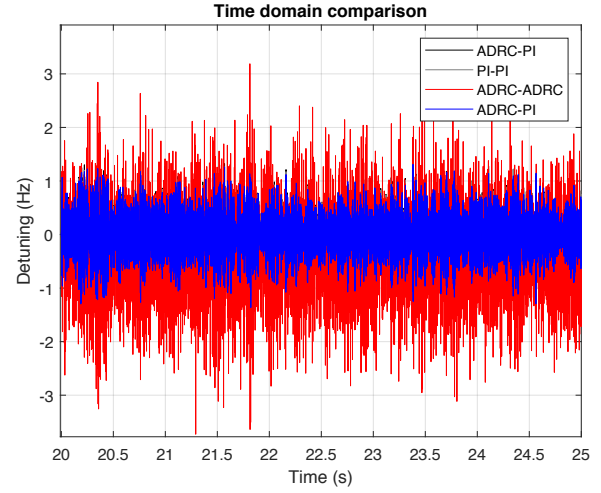


Figure 4: Microphonics control in the time domain. ADRC-PI, PI-PI and ADRC-PI/AFF signals are overlapping.

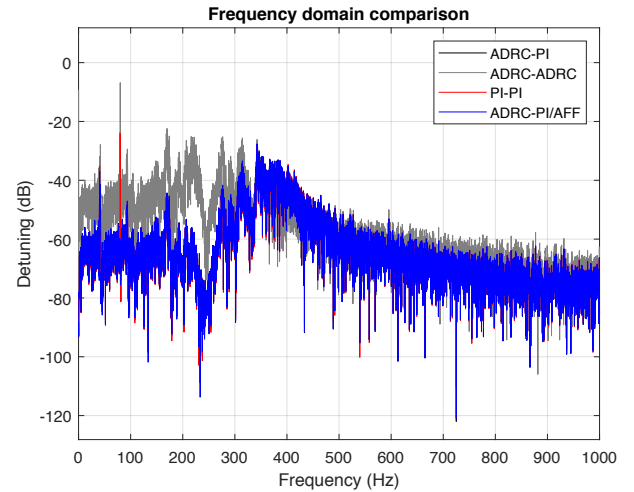


Figure 5: Microphonics control in the frequency domain

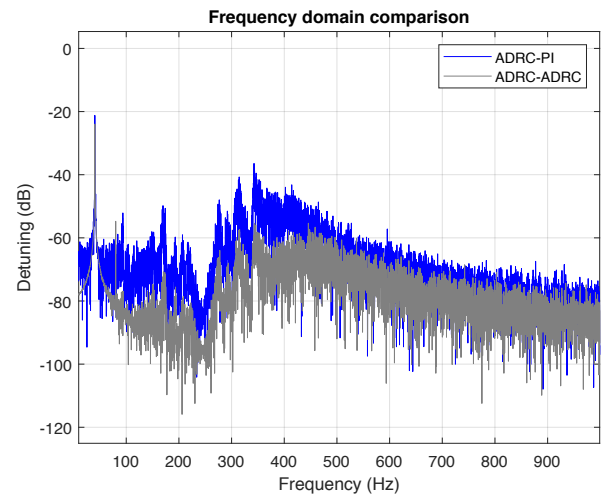


Figure 6: Microphonics control in the frequency domain without tuner time delay

for the first control loop. However, in the control loop for the detuning reduction, the results are not so good. The problem is the tuning of the parameters of the ADRC controller (observer and control gains) for stabilizing the loop, due to the delay introduced by the tuner. This delay has a great impact in the ADRC performance, limiting its effect. As it is shown in Figure 6, the ADRC controller gives very good results, reducing the delay effect.

On the other hand, the delay and the interaction of the ADRC controllers in both loops (Scenario 4) cause the instability of the system.

Finally, the non-collocated control problem is considered supposing different dynamics for the mechanical perturbations in the cavity and the actuator's effect, the piezo-tuner. The control schemes considered have been able to work in the particular configuration studied. Nonetheless, more analysis are needed, since the controllability or observability loss due to the non-collocated control problem can lead to malfunction controllers.

CONCLUSIONS

The use of virtual cavities facilitates the improvement of its support systems and, in particular following the model design approach, the test of different control algorithms for stabilizing the RF signals and the resonance frequency against perturbations. Taking into account the results presented in this work, the ADRC control strategy, which has been successfully tested in previous works, and its combination with other control techniques shows very good results in the simulation test, which fuels further studies in the future. The preliminary simulation results show that delay has an important impact in the performance of the microphonics reduction.

Consequently, the reduction of the delay effect in the system performance, implementing adequate control schemes [13, 14], is a problem to consider in future works. Other problem to consider is the non-collocated control problem, that is, performance considerations taking into account that perturbation sources and correction actions are located physically at different points.

In any case, those good (and future) results, should be validated in a second phase, using the FPGA based HIL system, since provides a more realistic simulator and will meet the system's dynamics in time and will allow testing the controller's hardware implementation as well as its in-time performance. This procedure will lead to a better performance of the Tesla cavity under analysis.

However, as a more general consideration, the use of open source cavity models as reference for testing of control algorithms will give information not only valid for a particular system, but general insights for selecting the most promising control algorithms to all the community.

ACKNOWLEDGEMENT

The authors are very grateful for the partial support of this work by the projects DPI2017-82373-R (Spanish Ministry of the Economy, Industry and Competitiveness) and PIT30 (ELKARTEK, Program of the Basque Government).

REFERENCES

- [1] A. Bellandi, J. Branlard, H. Schlarb, C. Schmidt, S. Pfeiffer, A. Nawaz, W. Cichalewski, R. Rybaniec, Simulation of microphonic effects in high QL TESLA cavities during CW operations, LLRF Workshop 2017 (LLRF2017), rXiv:1803.09038 [physics.acc-ph]
- [2] Pablo Echevarria, Beñ at Garcia, Josu Jugo, Axel Neumann, Andriy Ushakov, Simulation of Quench Detection Algorithms for Helmholtz Zentrum Berlin SRF Cavities, 10th Int. Particle Accelerator Conf.(IPAC'19), Melbourne, Australia, 19-24 May 2019, pp. 2834-2837.
- [3] Pablo Echevarria, Eukeni Aldekoa, Josu Jugo, Axel Neumann, Andriy Ushakov, and Jens Knobloch, Superconducting radio-frequency virtual cavity for control algorithms debugging editors-pick Review of Scientific Instruments 89, 084706 (2018); <https://doi.org/10.1063/1.5041079>
- [4] C. Serrano, L. Doolittle, V. K. Vytla, Cryomodule-on-Chip Simulation Engine, 16th Int. Conf. on Accelerator and Large Experimental Control Systems (ICALEPCS2017), doi: 10.18429/JACoW-ICALEPCS2017-TUAPL06
- [5] J. Branlard, LLRF Controls and RF Operation, 19th International Conference on RF Superconductivity SRF2019, June 27-29, 2019
- [6] T. Schilcher, Ph.D. thesis, Universitat Hamburg, 1998.
- [7] A. Neumann, W. Anders, O. Kugeler, and J. Knobloch, Analysis and active compensation of microphonics in continuous wave narrow-bandwidth superconducting cavities, Phys. Rev. ST Accel. Beams 13, 082001 (2010)
- [8] John Vincent, Dan Morris, Nathan Usher, Zhiqiang Gao, Shen Zhao, Achille Nicoletti, Qinling Zheng, On active disturbance rejection based control design for superconducting RF cavities, Nuclear Instruments and Methods in Physics Research Section A: Accelerators, Spectrometers, Detectors and Associated Equipment Volume 643, Issue 1, 1 July 2011, Pages 11-16.
- [9] Widrow, B. and S.D. Stearns (1985). Adaptive signal processing. Prentice-Hall International.
- [10] Nilanjan Banerjee, Georg Hoffstaetter, Matthias Liepe, Peter Quigley, and Zeyu Zhou, Active suppression of microphonics detuning in high QL cavities, Phys. Rev. Accel. Beams 22 22, 052002 (2019)
- [11] Shen Zhao, Nathan Usher, Dan Morris, Zhihong Zheng, Application of Active Disturbance Rejection Control in Superconducting Radio Frequency Cavities Proceeding of LLRF 2013, California, USA 2013.
- [12] Zheqiao Geng, Superconducting Cavity Control and Model Identification Based on Active Disturbance Rejection Control, IEEE Trans. on Nuclear Science, Vol. 64, No. 3, March 2017
- [13] S. Zhao et al., Modified active disturbance rejection control for time-delay systems, ISA Transactions, 2013,
- [14] Caifen Fun, Wen Tan, Control of unstable processes with time delays via ADRC, ISA Transactions Volume 71, Part 2, November 2017, Pages 530-541.